

# Metabolomics profiling of the free and total oxidised lipids in urine by LC-MS/MS: application in patients with rheumatoid arthritis

Junzeng Fu<sup>1,2</sup> · Johannes C. Schoeman<sup>1,3</sup> · Amy C. Harms<sup>1,3</sup> · Herman A. van Wietmarschen<sup>2,4</sup> · Rob J. Vreeken<sup>1,3,5</sup> · Ruud Berger<sup>1,3</sup> · Bart V. J. Cuppen<sup>6</sup> · Floris P. J. G. Lafeber<sup>6</sup> · Jan van der Greef<sup>1,2,3,4</sup> · Thomas Hankemeier<sup>1,3</sup>

Received: 5 May 2016 / Revised: 13 June 2016 / Accepted: 22 June 2016 / Published online: 12 July 2016  
© The Author(s) 2016. This article is published with open access at Springerlink.com

**Abstract** Oxidised lipids, covering enzymatic and auto-oxidation-synthesised mediators, are important signalling metabolites in inflammation while also providing a readout for oxidative stress, both of which are prominent physiological processes in a plethora of diseases. Excretion of these metabolites via urine is enhanced through the phase-II conjugation with glucuronic acid, resulting in increased hydrophilicity of these lipid mediators. Here, we developed a bovine liver- $\beta$ -glucuronidase hydrolysing sample preparation method, using liquid chromatography coupled to tandem mass spectrometry

to analyse the total urinary oxidised lipid profile including the prostaglandins, isoprostanes, dihydroxy-fatty acids, hydroxy-fatty acids and the nitro-fatty acids. Our method detected more than 70 oxidised lipids biosynthesised from two non-enzymatic and three enzymatic pathways in urine samples. The total oxidised lipid profiling method was developed and validated for human urine and was demonstrated for urine samples from patients with rheumatoid arthritis. Pro-inflammatory mediators  $\text{PGF}_{2\alpha}$  and  $\text{PGF}_{3\alpha}$  and oxidative stress markers  $\text{iPF}_{2\alpha}$ -IV, 11-HETE and 14-HDoHE were positively associated with improvement of disease activity score. Furthermore, the anti-inflammatory nitro-fatty acids were negatively associated with baseline disease activity. In conclusion, the developed methodology expands the current metabolic profiling of oxidised lipids in urine, and its application will enhance our understanding of the role these bioactive metabolites play in health and disease.

Junzeng Fu and Johannes C. Schoeman contributed equally to this work.

**Electronic supplementary material** The online version of this article (doi:10.1007/s00216-016-9742-2) contains supplementary material, which is available to authorized users.

✉ Junzeng Fu  
j.fu@lacdr.leidenuniv.nl

- <sup>1</sup> Department of Analytical Biosciences, Leiden Academic Center for Drug Research, Leiden University, Einsteinweg 55, 2333 CC Leiden, The Netherlands
- <sup>2</sup> Sino-Dutch Center for Preventive and Personalized Medicine, P.O. Box 360, 3700 AJ Zeist, The Netherlands
- <sup>3</sup> Netherlands Metabolomics Centre, Leiden University, Einsteinweg 55, 2333 CC Leiden, The Netherlands
- <sup>4</sup> TNO, Netherlands Organization for Applied Scientific Research, Microbiology and Systems Biology, P.O. Box 360, 3700 AJ Zeist, The Netherlands
- <sup>5</sup> Present address: Discovery Sciences, Janssen R&D, Turnhoutseweg 30, 2340 Beerse, Belgium
- <sup>6</sup> Rheumatology and Clinical Immunology, University Medical Center Utrecht, F02.127, Heidelberglaan 100, 3584 CX Utrecht, The Netherlands

**Keywords** LC-MS/MS · Metabolomics · Oxidized lipids · Urine ·  $\beta$ -glucuronidase

## Introduction

Oxidised lipids are important signalling mediators in health and disease, capable of providing quantitative readouts relating to inflammatory and oxidative stress status. The de novo synthesis of oxidised lipids can be broadly divided into enzymatic and auto-oxidation pathways. The auto-oxidation pathway of oxidised lipids is interlinked with reactive oxygen species (ROS) or reactive nitrogen species (RNS), leading to the peroxidation of fatty acids in membrane-bound phospholipids and producing the isoprostanes (IsoPs) [1, 2] or nitro-

fatty acids (NO<sub>2</sub>-FAs) [3]. The lipid peroxidation readout from IsoPs are considered the golden standard for measuring oxidative stress in biological systems [4, 5]. Interestingly, NO<sub>2</sub>-FAs potentiate diverse anti-inflammatory signalling actions regarded as beneficial within health and disease [3]. These peroxidised lipids impair membrane and organelle integrity and are subsequently excreted from the cell into systemic circulation via cellular repair mechanisms [1].

The enzymatic routes include: (i) cyclooxygenase-I/II (COX-I/II), synthesising the prostaglandins (PGs); (ii) 5-/12-/15-lipoxygenase (5-/12-/15-LOX), synthesising leukotrienes, lipoxins and hydroxyl-fatty acids; and lastly, (iii) cytochrome P450 (CYP450) responsible for the synthesis of epoxy-fatty acids and dihydroxy-fatty acids [6]. These enzymatically oxidised lipids are synthesised locally from essential free fatty acids and act as signalling mediators in immune modulation and inflammatory responses [6–9]. Due to the potent biological signalling activity of enzymatically oxidised lipids, the active mediators are short-lived in systemic circulation where they are actively metabolised prior to excretion [10]. Thus taking serum and/or plasma as a representative snapshot of the systemic circulation might not be the most suitable approach to study the oxidised lipid profile. Urine, on the other hand, is a non-invasive bio-fluid, which contains the collected excreted downstream metabolic products. These downstream metabolites provide an enriched systemic readout and are indicative of the presence of the active upstream mediators.

Urine does present some sample specific complications for analysis, such as rather large variations in metabolite concentration, limited solubilities of apolar metabolites and conjugation of some metabolites. These complexities are even more prominent during the analyses of lipid-like metabolites in urine. Due to the partial hydrophobic nature, oxidised lipids are often conjugated to increase their hydrophilicity, mainly by phase-II metabolism located in the liver [11]. Phase-II metabolism comprises different enzymatic conjugation reactions, with oxidised lipids most commonly conjugated with glucuronic acid (GlcA) via UDP-glucuronosyltransferases [12–18]. Effectively, the oxidised lipids can be excreted in different forms via urine: the unconjugated (free) and the conjugated species [14, 16]. Actually, the GlcA-conjugated oxidised lipids represent a more hydrophilic form of the metabolites.

Robust metabolic profiling of urinary oxidised lipids has been reported using either gas- or liquid chromatography coupled to mass spectrometry [4, 19–27]. However, these methods either detected metabolites in their free form (neglecting the conjugated forms) or focused on a subset of IsoPs and/or PGs. These methodologies lack the broad scope of compounds necessary for a more thorough understanding of disease pathophysiology. Two recent

methods reporting on the total (free + conjugated) IsoPs and PGs levels showed increasing urinary metabolite concentrations ranging from 36 to 100 % [15, 28], indicating the significant increases when measuring the total concentration, but these methods excluded the LOX and CYP450-oxidised lipid metabolites. Therefore, it is necessary to develop a method able to measure the total urinary oxidised lipids covering the three enzymatic synthesis routes as well as the auto-oxidation metabolites, broadening its biological range.

In the present study, we developed and validated robust methods for measuring both the free and total levels of oxidised lipids in human urine samples, covering the PGs, IsoPs, hydroxyl-fatty acids, epoxy-fatty acids, leukotrienes, lipoxins and NO<sub>2</sub>-FAs. To measure the total oxidised urinary profile, we investigated the suitability of three different  $\beta$ -glucuronidase enzymes derived from *Helix pomatia*, *Escherichia coli* and bovine liver. We evaluated these by determining the increase in free metabolites, metabolite stability and enzyme blank effect. Bovine liver derived  $\beta$ -glucuronidase was chosen as the preferred hydrolysing agent and was used in the total oxidised lipid method and validated concurrently with the free oxidised lipid method. Furthermore, we evaluated the benefit of total level oxidised lipid analyses in urine of rheumatoid arthritis patients. The methodology we established covers a broad scope of oxidised lipid, which enables further investigation of the function and mechanism of these lipids in both health and disease.

## Materials and methods

### Chemicals and reagents

Ultra-performance liquid chromatography (UPLC)-grade acetonitrile, isopropanol, methanol, ethyl acetate and purified water were purchased from Biosolve B.V. (Valkenswaard, the Netherlands). Acetic acid, ammonium hydroxide, ammonium acetate and 2-propanol were acquired from Sigma-Aldrich (Zwijndrecht, the Netherlands). Sodium dihydrogen phosphate dihydrate, sodium hydrogen phosphate and sodium acetate were obtained from Merck (Darmstadt, Germany).

### $\beta$ -glucuronidase enzymes

$\beta$ -glucuronidase (GUS) from (1) *H. pomatia* type H-2 (aqueous solution,  $\geq 85,000$  units/mL), (2) *E. coli* IX-A (lyophilised powder, 1,000,000–5,000,000 units/g) and (3) bovine liver B-1 (solid,  $\geq 1,000,000$  units/g), together with the exogenous substrate of GUS 4-methylumbelliferyl  $\beta$ -D-glucopyranoside (MUG) were purchased from Sigma-Aldrich Corporation (St. Louis, MO, USA).

### Standards and internal standard solutions

Standards and deuterated standards were purchased from Cayman Chemicals (Ann Arbor, MI, USA), Bio-mol (Plymouth Meeting, PA, USA) or Larodan (Malmö, Sweden). Standard and deuterated standard solutions were prepared in methanol containing butylated hydroxy-toluene (BHT) (0.2 mg BHT/EDTA), stored at  $-80\text{ }^{\circ}\text{C}$ . Electronic supplementary material (ESM) Table S1 lists an overview of the deuterated internal standards (ISTDs) used in this study.

### Urine sample collection

#### *Collection of control urine for method development*

Morning urine was obtained from ten volunteers (five males and five females) age 27 to 32. The urine samples were pooled, mixed and 400  $\mu\text{L}$  were aliquoted into 2 mL Eppendorf tubes and immediately stored at  $-80\text{ }^{\circ}\text{C}$  prior to extraction.

#### *Rheumatoid arthritis patients*

Oxidised lipid profiling was performed on urine samples derived from an observational study—BiOCURA [29]. In BiOCURA, rheumatoid arthritis (RA) patients eligible for biological disease-modifying anti-rheumatic drugs (bDMARDs) were recruited, and urine samples were collected at random times as baseline samples before initiating bDMARD therapy. Clinical parameters and demographic data were also collected at the start of the study as baseline information, including disease activity measured in 28 joints (DAS28), C-reactive protein (CRP), age, sex, BMI, smoking status, alcohol consumption and concomitant DMARDs. The study was approved by the ethics committee of the University Medical Centre Utrecht and the institutional review boards of the participating centres. Human material and human data were handled in accordance with the Declaration of Helsinki, and written informed consent was obtained from each patient.

Our analysis was restricted to the BiOCURA patients with a baseline (before bDMARDs treatment) disease activity score of  $>2.6$  and good or no drug response after 3 months with Etanercept (ETN) or Adalimumab (ADA) based on the EULAR response criteria. EULAR good response is defined as an improvement in DAS28  $>1.2$  and a present DAS28  $\leq 3.2$ , whereas a EULAR non-response is assigned to patients with an improvement of 0.6–1.2 with present DAS28  $> 5.1$  or patients with an improvement  $\leq 0.6$ . In the end, 40 subjects (20 good responders, 20 non-responders) with ETN and 40 subjects (20 good responders, 20 non-responders) with ADA were included in the present study. ETN and ADA are tumor

necrosis factor (TNF)- $\alpha$  inhibitors, which is the most widely used category of bDMARDs.

### Methodology development for optimising enzymatic hydrolysis

Hydrolysis conditions were optimised for each of the three GUSs following the approach in ESM Fig. S1. Parameters included enzyme concentration (1000, 1500 and 2000 U/sample), incubation temperature (37 and 55  $^{\circ}\text{C}$ ) and time (2, 6, 12 and 24 h). The obtained experimental results for the three enzymes were used to determine the optimal hydrolysing conditions.

#### *Enzymatic hydrolysing conditions*

Literature was used to guide the selection of the optimal hydrolysing conditions for the three selected candidate enzymes with regard to the used buffer composition and pH [18, 30, 31]. For both, *H. pomatia* and bovine liver GUS, a 200-mM acetate buffer (pH 4.5) was used for hydrolysis, and for *E. coli* GUS, a hydrolysis buffer of 75 mM phosphate buffer (pH 6.8) was used. As a sensitive GUS substrate, MUG was added into each urine sample as a positive control for monitoring GUS activity.

#### *Enzymatic hydrolysis procedure for GlcA-conjugated oxidised lipids*

Ice-thawed urine samples (400  $\mu\text{L}$  each) were immediately treated with 10  $\mu\text{L}$  antioxidants (0.2 mg BHT/EDTA) and spiked with 20  $\mu\text{L}$  ISTDs and 5  $\mu\text{L}$  MUG solution. Next, 200  $\mu\text{L}$  of the specific enzyme solution in its appropriate buffer was added to the sample, and the mixture was vortexed and incubated. After hydrolysis, samples were put on ice prior to oxidised lipid extraction.

### Total and free urinary oxidised lipid extraction

For both, total and free oxidised lipids, the extraction was performed by the same ethyl acetate liquid-liquid extraction (LLE) procedure. For the analyses of the free oxidised lipids, 400  $\mu\text{L}$  urine were spiked with 10  $\mu\text{L}$  antioxidants and 20  $\mu\text{L}$  ISTDs, similar to the description of enzymatic hydrolysed (total) samples in “Enzymatic hydrolysis procedure for GlcA-conjugated oxidised lipids”. Subsequently, 200  $\mu\text{L}$  citric acid/phosphate buffer (pH 3) was added to the total and free urine samples, and oxidised lipids were extracted by adding 1 mL ethyl acetate followed by shaking for 1 min. Samples were centrifuged at 13,000 rpm for 10 min (4  $^{\circ}\text{C}$ ), after which 800  $\mu\text{L}$  upper organic phase was transferred to a new Eppendorf tube. The LLE was repeated for a second time, and the collected organic phase was evaporated to dryness in Labconco CentriVap concentrator

(Kansas City, MO, USA). The residues were reconstituted with 30  $\mu$ L solution of 70 % methanol solution containing 100 nM 1-cyclohexyluriedo-3-dodecanoic acid (CUDA) as an external quality marker for the analysis. Afterwards, the extracts were centrifuged at 13,000 rpm for 5 min (4 °C) and transferred to LC autosampler vials.

### Lipid chromatography-mass spectrometry analyses (LC-MS/MS)

The complete oxidised lipid target lists and corresponding ISTDs divided per pathway are shown in ESM Table S2, S3, S4 and S5. The leukotrienes, hydroxyl-fatty acids, epoxy-fatty acids and lipoxins were analysed by high-performance liquid chromatography (Agilent 1260, San Jose, CA, USA) coupled to a triple-quadrupole mass spectrometer (Agilent 6460, San Jose, CA, USA), using an Ascentis® Express column (2.7  $\mu$ m, 2.1  $\times$  150 mm) as detailed in Strassburg et al. [32].

For adequate PG and IsoP isomer resolution, together with sensitive detection of the NO<sub>2</sub>-FAs, an optimised chromatographic method was developed in-house. UHPLC-MS/MS analysis was performed using the Shimadzu LCMS-8050 (Shimadzu, Japan) with a Kromasil EternityXT column (1.8  $\mu$ m, 50  $\times$  2.1 mm) maintained at 40 °C. The method used a three mobile-phase setup with: H<sub>2</sub>O with 5 mM ammonium acetate and 0.0625 % ammonium hydroxide (A), methanol with 0.2 % ammonium hydroxide (B) and isopropanol with 0.2 % ammonium hydroxide (C), with a flow rate of 0.6 mL/min. The injection volume was 10  $\mu$ L, and all analytes eluted during a 10-min ternary gradient with a starting percentage composition of 94.5:5:0.5 (A/B/C). A chromatographic gradient is provided in ESM Fig. S2.

The LCMS-8050 consisted of a triple-quadrupole mass spectrometer with a heated electrospray ionisation (ESI) source. In negative ion mode, the source parameters were as follows: the heat block temperature was 400 °C, with the heating gas at 250 °C and a flow of 10 L/min. The nebulising and drying gas had a flow rate of 3 and 10 L/min, respectively. The interface voltage was set at 4 kV with a temperature of 150 °C. The conversion dynode was set at 10 kV, and desolvation temperature was 250 °C. Analytes were detected in negative MRM mode.

### Method validation

The targeted profiling of oxidised lipids has previously been validated for plasma samples, and the performance characteristics linearity, intra- and inter-day precision and accuracy were reported [32]. In the present study, we used the same chromatography parameters in terms of the columns, mobile phase, gradient etc. Therefore, the current validation was performed to determine recovery, matrix effect and precision for the ISTDs for the reported extraction method.

### Creatinine analysis

Urine samples of RA patients were collected at a random time of day, therefore the amount of liquids consumed influenced the concentration of the oxidised lipids in the samples. To eliminate this influence, levels of urinary creatinine were used to correct for dilution. Creatinine levels were determined based on a fast creatinine (urinary) assay kit (item no. 500701, Cayman Chemical Company, Ann Arbor, MI, USA).

### Data processing and statistical analyses

Peak determination and peak area integration were performed with Mass Hunter Quantitative Analysis (Agilent, Version B.04.00) and LabSolutions (Shimadzu, Version 5.65). The obtained peak areas of targets were first corrected by appropriate ISTD and creatinine concentrations (mg/dL), then normalised by log transformation. After data pre-processing, categorical principal component analysis (CATPCA, ESM methods) [33] and multiple linear regressions (MLR) were applied to explore the relationships between oxidised lipids and clinical parameters. Cytoscape was used to visualise the associations [34]. All statistical analysis was performed using IBM SPSS Statistics 23.0 software (Chicago, IL, USA).

## Results

### Optimisation for the hydrolysis of IsoPs, PGs and NO<sub>2</sub>-FAs

For determining the optimal enzymatic deconjugation procedure for urinary oxidised lipids, three GUSs derived from *H. pomatia*, *E. coli* and bovine liver were investigated. During the method development, critical parameters including enzyme concentrations, hydrolysis temperature and time were optimised. In order to simplify the method optimisation, we focused on the quantification of a pre-selected panel of metabolites to evaluate the method performance, which covers the most studied IsoPs, PGs and NO<sub>2</sub>-FAs in human body fluids. The selected panel consisted of F-series IsoPs (8-iso-PGF<sub>2 $\alpha$</sub> , 8-iso-15(R)-PGF<sub>2 $\alpha$</sub>  and 8-iso-13,14-dihydro-PGF<sub>2 $\alpha$</sub> ), F- and E-series PGs (PGF<sub>2 $\alpha$</sub> , 13,14-dihydro-PGF<sub>2 $\alpha$</sub> , PGE<sub>1</sub> and PGE<sub>2</sub>) and two NO<sub>2</sub>-FAs mediators (NO<sub>2</sub>-linoleic acid and NO<sub>2</sub>-oleic acid) (see ESM Table S6).

For all three GUSs tested, the optimal conditions was 1000 U enzyme/400  $\mu$ L urine incubated at 37 °C for 2 h. No increase in metabolite levels were achieved through increasing the hydrolysis time beyond 2 h or from increasing the temperature (data not shown). Choosing the shortest possible hydrolysis time will also increase the throughput of the method. Figure 1 presents the increase (or decrease) of the concentration (as reflected by the changes of the peak area)

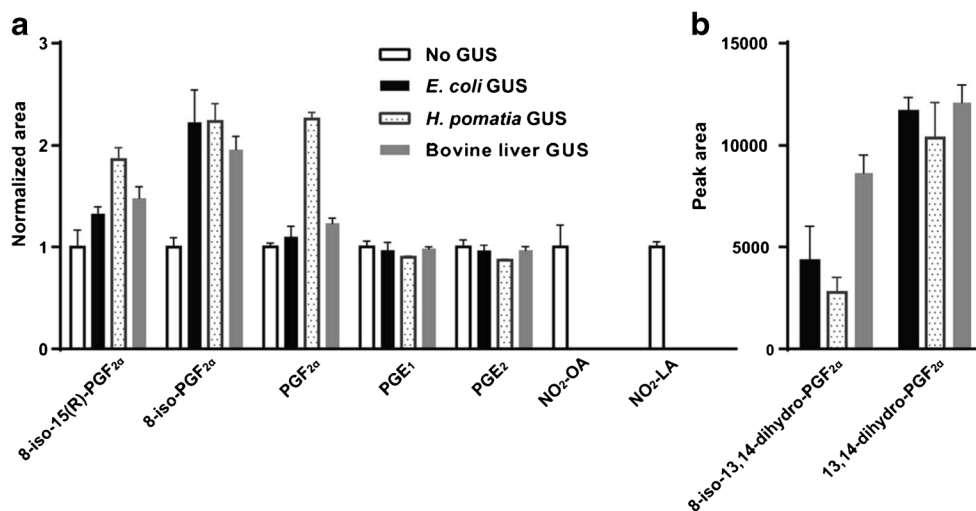


**Fig. 1** Changes in response of the selected panel of compounds in the urine samples after 2 h enzymatic hydrolysis (at 37 °C with *E. coli*, *H. pomatia* or bovine liver GUS) compared with non-hydrolysed samples (no GUS). **A** y-axis represents the normalised peak area of a metabolite

normalised to the mean area of the corresponding peak in non-hydrolysed urine. **B** y-axis represents the peak area without normalisation since 8-iso-13,14-dihydro-PGF<sub>2α</sub> and 13,14-dihydro-PGF<sub>2α</sub> were exclusively detected in GUS-hydrolysed urine. Error bars indicate standard deviation

in the sample after hydrolysis compared with prior to the hydrolysis for a selected panel of compounds. Significant increases were observed for the F-series IsoPs—all three enzymes increased the metabolite levels by more than 50 %. Some downstream metabolites, 8-iso-13,14-dihydro-PGF<sub>2α</sub> and 13,14-dihydro-PGF<sub>2α</sub>, were exclusively detected after GUS hydrolysis (Fig. 1b). No significant increase in the E-series PGs compared with the free levels were found after GUS hydrolysis. The NO<sub>2</sub>-FAs mediators could not be analysed after hydrolysis due to their extreme temperature and enzymatic lability (see below for further discussion). No significant differences in the hydrolysis efficiency were found between the three GUSs for the pre-selected panel of compounds. Our final choice of the GUS for our protocol was finally made based on encountered blank effects of GUSs and metabolite stability in presence of the GUS (see below).

#### The enzyme blank effect

We identified an important and so far unreported observation related to an oxidised lipid background present within the three GUSs, especially for *H. pomatia*. Evaluation of the enzyme blank samples, which consisted of water following the GUS hydrolyses sample workup, revealed the presence of an oxidised lipid background. In Fig. 2, we show the LC-MS/MS trace for PGF<sub>2α</sub> and PGE<sub>2</sub> in the non-hydrolysed urine sample, GUS blank samples and procedure blank sample (water sample extracted by LLE, no enzyme added). Figure 2a shows there is no signal for PGF<sub>2α</sub> in the procedure blank sample while a high level of PGF<sub>2α</sub> were found especially in the *H. pomatia* GUS blank sample. The levels of PGF<sub>2α</sub> in *E. coli* and bovine liver GUS samples were lower compared

with the high PGF<sub>2α</sub> background present in *H. pomatia*. Similar observations are made for PGE<sub>2</sub> (Fig. 2b). For the selected panel of oxidised lipids, the enzyme blank effect is presented by the area ratio between the blank enzyme sample and the hydrolysed sample at 2 h ( $\text{Area}_{\text{in enzyme blank sample}} / \text{Area}_{\text{in 2 h hydrolysed sample}}$ ). Inspection of the complete IsoP, PG and NO<sub>2</sub>-FA target panel found that *H. pomatia* GUS contained the highest blank effect compared with *E. coli* and bovine liver (see ESM Table S7). Based on this observation, *H. pomatia* was not considered a suitable GUS candidate to measure the total urinary oxidised lipid profile.

#### Internal standard stability

Beside the enzyme blank effect, the stability of the ISTDs during the 2 h incubation at 37 °C was investigated as representative for their respective endogenous metabolite classes. The percentage change for the ISTDs treated with the three different enzymes in 2 h compared with 0 h were determined and are shown in Fig. 3. ISTDs representing the F-series PGs and IsoPs were identified as stable at 37 °C, over 2 h with the addition of an enzyme included, showing less than 10 % change in their levels. However, the E- and D-series PG ISTDs showed temperature sensitivity, especially PGD<sub>2</sub>-d4. Reversely, the A-series PG ISTD PGA<sub>2</sub>-d4 showed increasing concentrations, possibly due to PGD<sub>2</sub>-d4 spontaneous dehydration forming PGA<sub>2</sub>-d4. The 10-NO<sub>2</sub>-Oleic acid d17 (NO<sub>2</sub>-FAs ISTD) showed hypersensitivity to hydrolysis conditions (buffer and temperature), showing a 40 % decrease in levels within 2 h compared with non-hydrolysed sample. Furthermore, the addition of all three enzymes resulted in a more pronounced decrease (70 to 90 %), explaining the above-mentioned decrease of endogenous NO<sub>2</sub>-FAs during enzymatic hydrolyses. Overall,

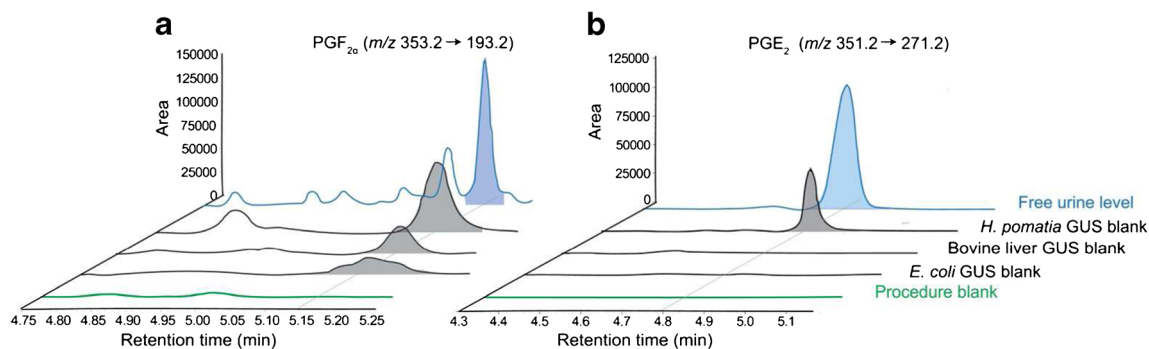


**Fig. 2** The enzymatic oxidised lipid background (enzyme blank effect). LC-MS/MS chromatograms representing the procedure blank (*green*), followed by the three enzyme blank samples (*E. coli*, bovine liver and *H. pomatia*), and the free urine levels (*blue*) are overlaid for (A)  $\text{PGF}_{2\alpha}$

and (B)  $\text{PGE}_2$ , respectively. *H. pomatia* GUS shows a high oxidised lipid background. Samples were monitored for  $\text{PGF}_{2\alpha}$  ( $m/z$  353.2  $\rightarrow$  193.2) and  $\text{PGE}_2$  ( $m/z$  351.2  $\rightarrow$  271.2)

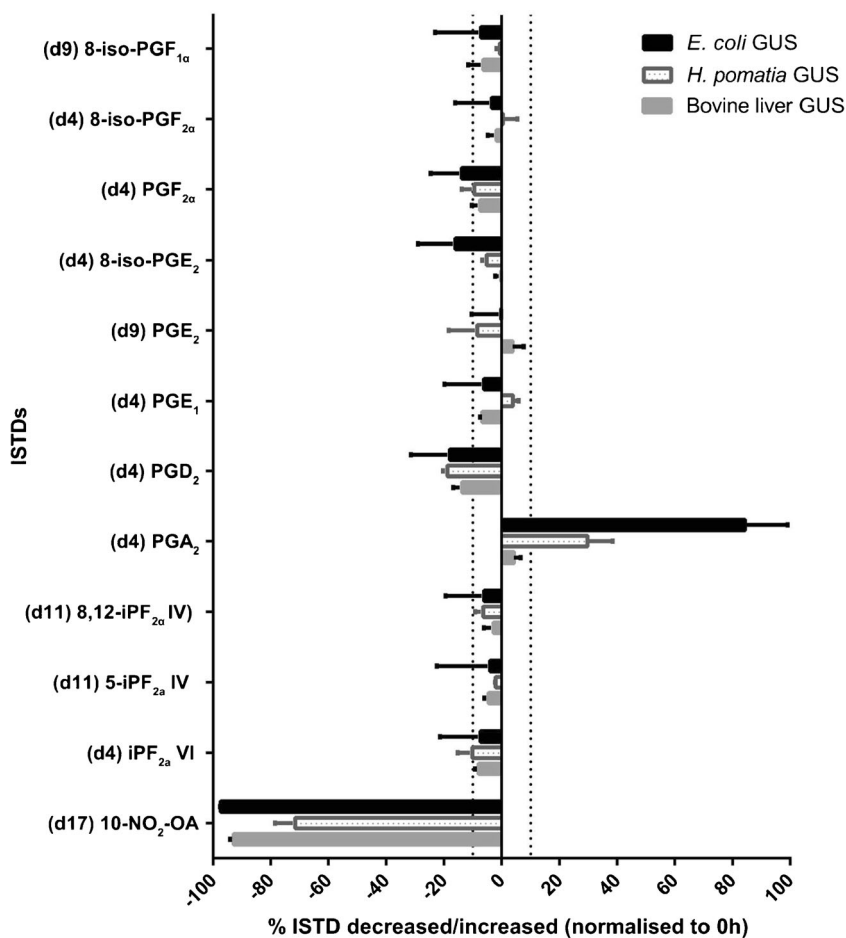
the hydrolysis using GUS from *E. coli* showed the largest percentage change for the evaluated ISTDs, suggesting that the 75 mM phosphate buffer (pH 6.8) or *E. coli* GUS affect compound stability. Although, bovine liver GUS showed similar ISTD stability compared with *H. pomatia*, the latter's significant enzyme blank effect led to bovine liver being chosen as our preferred hydrolysing enzyme. Furthermore, bovine liver GUS also resulted in the inclusion of D- and A-series PGs in the target list. Therefore, we

chose bovine liver-derived GUS hydrolysing at 37 °C for 2 h as the optimal procedure for analysing the urinary oxidised lipid profile.

### Increasing the metabolite scope

Using the optimised bovine liver hydrolyses method, we investigated the potential to broaden the scope of the measurable oxidised urinary lipid profile. We targeted the metabolites from

**Fig. 3** The stability of the IsoP, PG and  $\text{NO}_2$ -FA ISTDs during the 2-h hydrolyses. The percentage changes of ISTD levels (compare 2 with 0 h) were investigated to evaluate the stability of each ISTD. Overall, ISTDs with bovine liver GUS hydrolysis indicated the highest degree of stability. The vertical dotted lines indicate 10 % change. x-axis indicates percentage changes of ISTD areas between 2 and 0 h ( $\text{area}_{2\text{ h-ISTD}}/\text{area}_{0\text{ h-ISTD}} \times 100\%$ ). Error bars indicate standard deviation



auto-oxidation, COX, LOX and CYP450 pathways and compared the amount of free oxidised lipids (from non-hydrolysed urine) with the total amount of oxidised lipids (from hydrolysed urine). There were 51 metabolites detected in both hydrolysed and non-hydrolysed samples, of which 23 metabolites were significantly increased by hydrolysis. More importantly, 27 additional oxidised lipids were detected exclusively in the total oxidised lipid analysis (Table 1). As shown in Table 1, we were able to increase the scope of the method by using an enzymatic hydrolysis approach to measure the total urinary oxidised lipid signature, providing a more complete picture for biological interpretation.

### Method validation

Validation measurements were performed using pooled urine as a sample matrix. Recovery, matrix effect and batch-to-batch precision were determined.

### Recovery and ion suppression

The performances of the analytical methods (free and total oxidised lipid profiling) with respect to recovery (of the free forms) and ion suppression were validated for those metabolites which were available as deuterium-labelled compounds and which were usually used as ISTDs. For determining recoveries, samples were independently spiked before or spiked after the extraction procedure with ISTDs, and the area ratios between these samples ( $\text{Area}_{\text{spike before}}/\text{Area}_{\text{spike after}}$ ) were calculated as the recoveries. Figure 4a demonstrates that recoveries are from 85 to 115 % for most ISTDs, indicating the effectiveness of both procedures to extract the oxidised metabolome from urine samples. The non-hydrolysed samples (free levels) with a simpler sample handling procedure showed slightly higher recoveries compared with the hydrolysed procedure (total levels) except for the nitro-fatty acid

**Table 1** Urinary oxidised lipids measured by bovine liver GUS hydrolysis and non-hydrolysis methods

	RNS	ROS	COX	LOX	CYP450
Detected in both GUS-hydrolysed and GUS-non-hydrolysed urine		11-HDoHE*	13,14-dihydro-15-keto-PGE <sub>2</sub> *	12S-HEPE	12,13-DiHOME*
		14-HDoHE	15-keto-PGF <sub>1α</sub>	20-carboxy-LTB <sub>4</sub> <sup>#</sup>	12,13-EpOME*
		5-iPF <sub>2α</sub> -VI*	2,3-dinor-11b-PGF <sub>2α</sub> *	5S,6R-LipoxinA <sub>4</sub>	14,15-DiHETrE*
		8,12-iPF <sub>2α</sub> -IV*	2,3-dinor-8-iso-PGF <sub>2α</sub> *	11-HETE	8,9-DiHETrE*
		8-iso-15(R)-PGF <sub>2α</sub> *	20-hydroxy-PGE <sub>2</sub> <sup>#</sup>	11-trans-LTD <sub>4</sub> <sup>#</sup>	9,10-DiHOME*
		8-iso-15-keto-PGF <sub>2α</sub> *	Δ12-PGJ <sub>2</sub> *	12-HETE	9,10-EpOME*
		8-iso-PGE <sub>1</sub> <sup>#</sup>	Δ17, 6-ketoPGF <sub>1α</sub> *	13-HODE*	
		8-iso-PGE <sub>2</sub>	PGA <sub>2</sub>	13-KODE	
		8-iso-PGF <sub>1α</sub>	PGD <sub>1</sub> <sup>#</sup>	15-HETE*	
		8-iso-PGF <sub>2α</sub> *	PGD <sub>2</sub> <sup>#</sup>	5-HETE	
			PGE <sub>1</sub> <sup>#</sup>	9,10,13-TriHOME*	
			PGE <sub>2</sub>	9,12,13-TriHOME*	
			PGE <sub>3</sub>	9-HODE	
			PGF <sub>1α</sub>	9-HOTrE	
			PGF <sub>2α</sub> *	9-KODE	
			PGF <sub>3α</sub>	LTD <sub>4</sub> *	
			PGJ <sub>2</sub> <sup>#</sup>		
		Tetranor-PGEM <sup>#</sup>			
Detected in GUS hydrolysed urine exclusively		10-HDoHE	13_14-dihydro-PGF <sub>2α</sub>	15S-HETrE	20-HETE
		8-iso-13,14-dihydro-PGF <sub>2α</sub>	13,14-dihydro-15-keto-PGD <sub>2</sub>	15-HpETE	12,13-DiHODE
		8-iso-15-keto-PGF <sub>2β</sub>	13,14-dihydro-15-keto-PGF <sub>2α</sub>	5S,15S-DiHETE	19,20-DiHDPA
		9-HETE	15-deoxy-delta-12,14-PGD <sub>2</sub>	5S,6S-Lipoxin A <sub>4</sub>	11,12-DiHETrE
			15-keto-PGF <sub>2α</sub>	5S-HEPE	11,12-EpETrE
			16-HDoHE	5S-HpETE	14,15-DiHETE
			bicyclo-PGE <sub>2</sub>	9-HEPE	17,18-DiHETE
		PGK <sub>2</sub>		5,6-DiHETrE	
Detected in non-hydrolysed urine exclusively	NO <sub>2</sub> -αLA				
	NO <sub>2</sub> -LA				
	NO <sub>2</sub> -OA				

\*Significantly increased with hydrolysis; <sup>#</sup> significantly decreased with hydrolysis

ISTD (10-NO<sub>2</sub>-oleic acid-d17 as discussed in “Internal standard stability”).

To determine the ion suppression caused by the presence of compounds of the matrix, ISTD areas in urine samples spiked after the total and free oxidised lipid extractions were compared with the ISTD areas in injection solution. Ion suppression values shown in Fig. 4b ranged between 0.5 and 1 for most of the metabolites; values below 1 indicate the presence of ion suppression caused by co-eluting compounds from the urine matrix that were not removed by the sample preparation and that affect the ionisation of those targeted metabolites [35]. Three ISTDs with high ion suppression (lower than 0.5) were PGA<sub>2</sub>-d4, 6-ketoPGF<sub>1</sub>-d4 and TBX<sub>2</sub>-d4. However, ion suppression effects are corrected through the deuterated ISTD normalisation ( $\text{Area}_{\text{metabolite}}/\text{Area}_{\text{ISTD}}$ ) as both the metabolite and its corresponding ISTD experience similar ion suppression.

#### Precision and batch-to-batch effect

To be able to reproducibly and accurately report the oxidised lipid metabolome from patient urine samples, it is important to estimate the analytical variation. Therefore, the intra-batch precision and inter-batch

variability were assessed for all endogenous oxidised lipids. Precision is dependent on extraction reproducibility, injection variation and detector stability, while the inter-batch variability is influenced by the robustness of the chromatography and instrument stability across different measurement days ( $n = 3$ ).

In ESM Fig. S3a, the precision (intra-batch RSD) and in ESM Fig. S3b, the batch-to-batch effect (inter-batch RSD) of endogenous metabolites obtained from hydrolysed/non-hydrolysed urine samples are shown. Investigating the precision for the non-hydrolysed procedure showed that 59 % of metabolites had the RSD < 15 %, with a further 25 % of metabolites having a RSD between 15 and 30 %. The hydrolysed procedure showed improved precision with 66 % of metabolites having the RSD < 15 % and 29 % of metabolites having a RSD between 15 and 30 %. The increased precision observed in the hydrolysed procedure can be attributed to increased metabolite concentrations, leading to more accurate detection, while the higher variation in the non-hydrolysed procedure was predominantly driven by low abundant compounds. Both procedures performed equally well in batch-to-batch effects, indicative of a stable and reproducible LC-MS analyses across three measurement days.

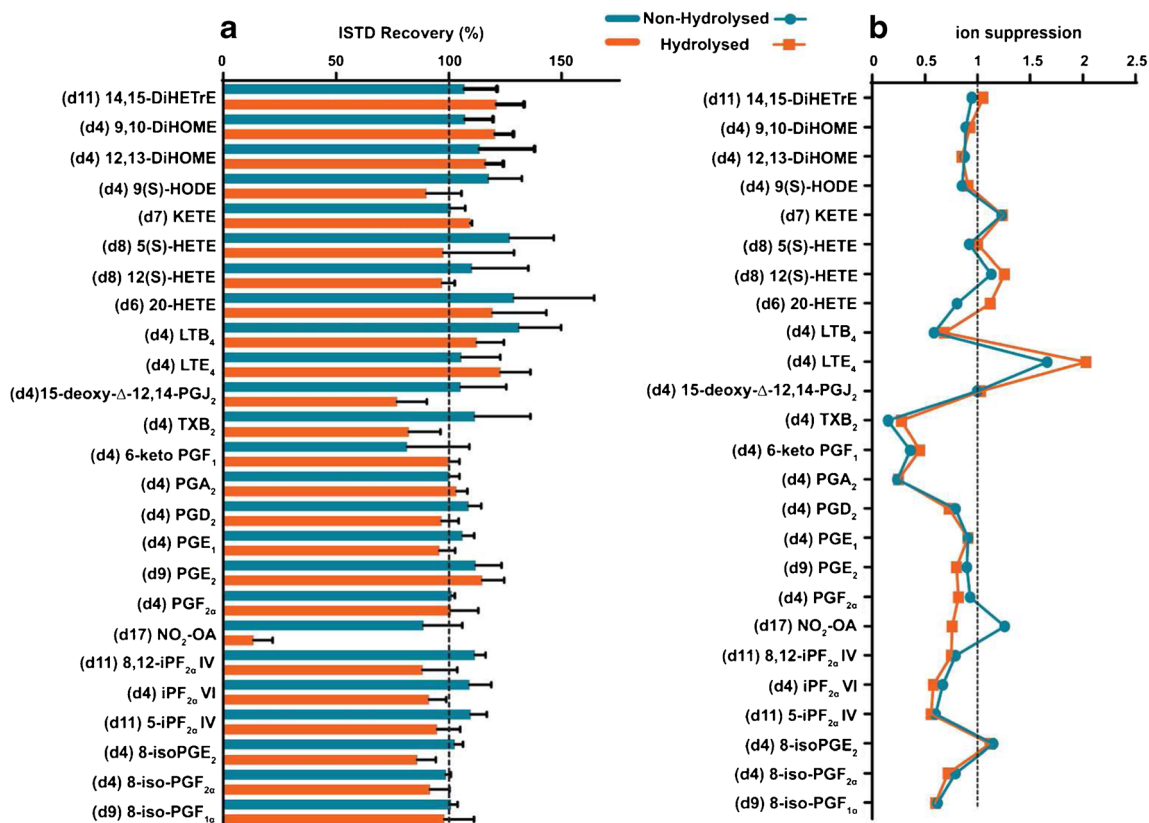


**Fig. 4** Performance characteristics of sample preparation. Deuterium-labelled ISTDs were evaluated for (A) recovery and (B) ion suppression; values below 1 indicate presence of ion suppression (B)



## Application

### Subjects

For the present study, baseline urine samples from RA patients who were treated with TNF- $\alpha$  inhibitors (ETN or ADA) were selected based on good response or non-response after 3 months of therapy. The baseline characteristics of 80 patients are shown in Table 2. Subjects had a mean age of 53.8 years, a median disease duration of 5 years and had previously taken a mean of two concomitant disease-modifying anti-rheumatic drugs (co-DMARDs). Subjects were mainly female (58 females, 22 males). Good responders had higher baseline DAS28 ( $4.8 \pm 0.9$  compared with  $4.2 \pm 1.1$ ,  $P = 0.006$ ) and C-reactive protein (CRP) levels ( $8 \pm 11$  compared with  $5 \pm 7$ ,  $P = 0.04$ ) compared with the non-responders. There were no significant differences between the other parameters.

### Detection of oxidised lipids in human urine

Applying total and free oxidised lipid profiling to randomly collected urine samples, we are able to detect 67 metabolites in hydrolysed urine samples and 44 in non-hydrolysed urine samples. There were 97 % total and 95 % free oxidised lipid metabolites measured with a RSD < 30 % (see ESM Table S8). Because the total oxidised lipid profiling provides a larger scope of metabolites, we focused on the total urinary oxidised lipid profiles (after hydrolysis), in addition to the free NO<sub>2</sub>-FAs levels measured in the analyses without hydrolysis in the subsequent data analyses and interpretation.

### Relationships between total oxidised lipids profiling and RA-associated parameters

To investigate the relationship between RA-associated parameters and total oxidised lipid levels, repeated assessments using multiple linear regression (MLR) models were performed on individual metabolite. Confounding factors (age, sex, BMI, smoking status, alcohol consumption, co-DMARDs) and RA-associated parameters (baseline DAS28, CRP and DAS28 improvement) were added into MLR as independent variables, and the oxidised lipid level was set as the dependent variable. RA-associated parameters which were correlated with oxidised lipid levels ( $P < 0.10$ ) were selected (Table S9) and are visualised by Cytoscape in Fig. 5. CRP showed a positive correlation with 16-HDoHE ( $P = 0.027$ ) and a negative correlation with PGD<sub>3</sub> ( $P = 0.026$ ); DAS 28 showed a positive association with 14,15-DiHETE ( $P = 0.036$ ) and 5S, 6R-LipoxinA4 ( $P = 0.005$ ); DAS28 improvement ( $\text{DAS28}_{\text{month 0}} - \text{DAS28}_{\text{month 3}}$ ) showed significantly positive association with PGF<sub>3 $\alpha$</sub>  ( $P = 0.017$ ), PGF<sub>2 $\alpha$</sub>  ( $P = 0.018$ ), iPF<sub>2a</sub> IV ( $P = 0.021$ ), 11,12-EpETrE ( $P = 0.040$ ), 11-HETE ( $P = 0.019$ ), 14,15-DiHETrE ( $P = 0.017$ ) and 14-HDoHE ( $P = 0.033$ ). Since NO<sub>2</sub>-FAs were labile in the hydrolysing procedure, we included the free NO<sub>2</sub>- $\alpha$ LA, NO<sub>2</sub>-LA and NO<sub>2</sub>-OA levels during the MLR. These three metabolites were all negatively associated with baseline DAS28 ( $P < 0.05$ ).

## Discussion

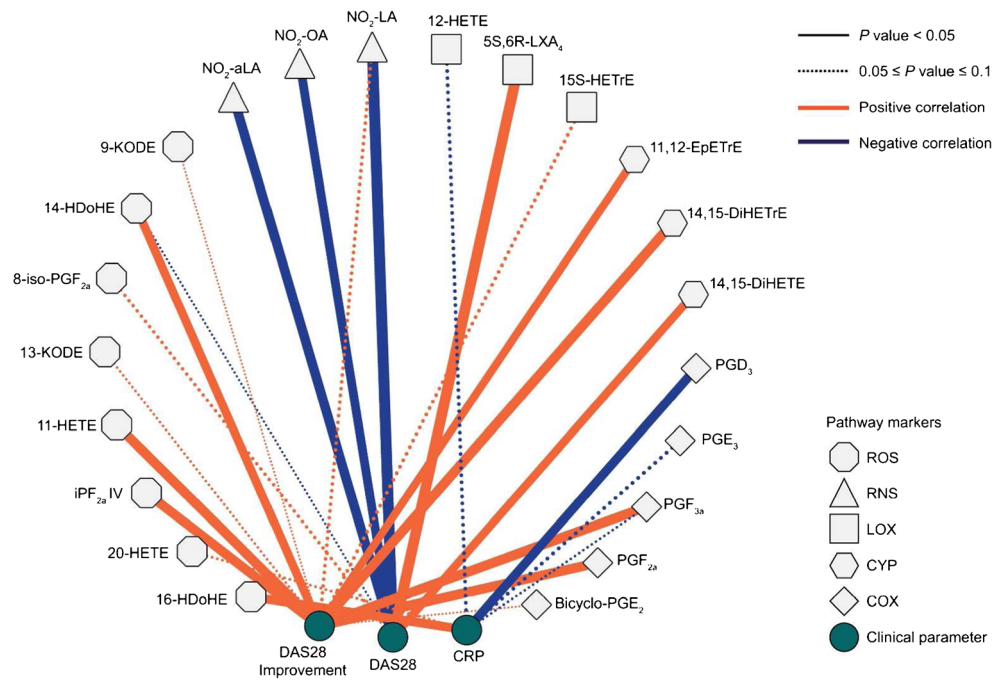
In the present study, we optimised and validated a GUS-based hydrolysis method to evaluate the oxidised urinary lipid

**Table 2** Baseline characteristics of the study subjects ( $n = 80$ ), subdivided according to the therapeutic response at 3 months

	All subject ( $n = 80$ )	Non-response ( $n = 40$ )	Good response ( $n = 40$ )	$P$ value (good responders vs. non-responders)
Gender (female, $n$ (%))	58 (72.5)	31 (77.5)	27 (67.5)	0.453
Age (mean (SD))	53.8 (11.0)	52.7 (11.3)	55.1 (10.8)	0.461
Disease duration (median (IQR))	5 (8.0)	5 (7.0)	6 (9.0)	1.000
Smoking currently ( $n$ (%))	23 (28.7)	12 (30.0)	11 (27.5)	0.805
Alcohol >7 units/week ( $n$ (%))	16 (20.3)	5 (12.5)	11 (27.5)	0.099
BMI (mean (SD))	26.9 (5.3)	27.1 (5.0)	26.7 (5.6)	0.874
RF (positive, $n$ (%))	57 (71.3)	26 (65.0)	31 (77.5)	0.323
ACPA (positive, $n$ (%))	57 (71.3)	26 (65.0)	31 (77.5)	0.323
Baseline DAS28 (mean (SD))	4.5 (1.0)	4.2 (1.1)	4.8 (0.9)	<b>0.006</b>
CRP (median (IQR))	7 (10.0)	5 (8)	8 (11.0)	<b>0.045</b>

SD standard deviation, IQR interquartile range

**Fig. 5** Correlations between rheumatoid arthritis-associated clinical parameters and oxidised lipid levels with  $P < 0.10$  based on multiple linear regression analyses



profile. We demonstrated that the number of measured oxidised lipids were approximately twofold increased after hydrolysing with bovine liver-sourced GUS. Furthermore, we applied the method to urine samples from patients with RA and identified oxidised lipids associated with RA-associated parameters important in determining therapeutic response.

As a non-invasive biological matrix, urine is easily collected and can effectively be used as an oxidised lipids readout. However, urine does present some challenges including dilution effect (morning sample, 24 h sample, random sample), glucuronidation of metabolites with low solubility, and a high salt concentration etc. Although some of these challenges can be addressed with proper experimental planning and standardised sample collection procedures, the choice between analysing free or total levels of oxidised lipids still needs to be addressed. Thus, we developed a robust enzymatic method to hydrolyse the GlcA-conjugated oxidised lipids, obtaining the total oxidised lipid profile for urine samples. During the method development, we found an enzyme blank effect in the three candidate enzymes (see ESM Table S7) which needs to be minimised in order to avoid adding artefacts which could interfere with the biological interpretation of the results.

Several different GUS are available commercially for research purposes, with each enzyme having its own specific characteristics properties relating to substrate affinities and efficiency. Our choice of candidate enzymes was guided by selecting those previously reported in literature [18, 30, 31]. *H. pomatia* GUS was the most widely used enzyme but had a very prominent blank effect. The oxidised lipid background

might be derived from inadequate purifying and cleaning procedures used during enzyme extraction and isolation. While this might not be true for all forms of GUS derived from *H. pomatia*, we decided against the use of *H. pomatia* as the background might influence our biological interpretation of the data.

Comparing the total and free oxidised lipid profiles revealed increased levels, especially in the F-series IsoPs, F-series PGs, hydroxy-fatty acids and dihydroxy-fatty acids, while having minimal effect on E-series PGs in the total oxidised lipid profile. The lack of effect on the E-series PGs could be explained in a study done by Little et al., where they investigated the different human recombinant UDP-glucuronosyltransferases and found that only one isoform UGT2B7 was capable of forming PGE<sub>2</sub> glucuronide [17]. UGT2B7 were exclusively found in the colon, and faeces rather than urine might contain high levels of E-series glucuronide conjugates. The significant increase in LOX and CYP450 metabolites might be due to their increasing hydrophobic nature, with glucuronidation increasing their urinary excretion. Similar to our findings, Prakash et al., reported significant increase in the level of 20-HETE, an CYP450 metabolite in urine treated with  $\beta$ -glucuronidases, and they concluded that CYP450 metabolites are predominantly excreted in conjugated form [13]. Whereas the method reported by Newman et al. needed 4 mL of urine to measure the free CYP450-oxidised lipid metabolites [22], using our bovine liver hydrolysis method, we could evaluate the same CYP450 pathway metabolites by using ten times less urine.

Optimising the extraction and analyses of the anti-inflammatory NO<sub>2</sub>-FAs will aid us in studying the field of

nitrosative stress. A disappointing finding was our inability to accurately measure the total  $\text{NO}_2$ -FAs levels, due to their labile nature. Although, we were able to effectively measure the free  $\text{NO}_2$ - $\alpha$ LA,  $\text{NO}_2$ -LA and  $\text{NO}_2$ -OA levels in urine. In a work published by Salvatore et al., they showed the presence of cysteine- $\text{NO}_2$ -FA conjugates in urine and used a short chemical ( $\text{HgCl}_2$ ) hydrolysis procedure at 37 °C to measure its total levels [36]. Thus, to accurately measure the total  $\text{NO}_2$ -FA level identification of the primary conjugated form needs to be done, followed with optimised chemical hydrolyses.

For the urine samples from RA patients, which were collected at a random time of day, we used the urinary creatinine level for correcting the oxidised lipids for sample dilution. Samples were retrospectively divided into good or no responders to therapy based on EULAR response criteria. However, the subjects could not be separated into non-/good response groups based on their baseline urinary oxidised lipids profile and clinical parameters using categorical principle components analysis (CATPCA, score plot is shown in ESM Fig. S4). After correcting for confounding factors (age, sex, BMI, smoking status, alcohol consumption, co-DMARDs), the urinary oxidised lipid readout did show associations between inflammation and oxidative stress and clinical parameters (CRP, 3-month DAS28 improvement, baseline DAS28). C-reactive protein is an acute-phase inflammatory protein, which showed a positive correlation with 16-HDoHE, a docosahexaenoic acid (DHA) lipid peroxidation metabolite. DHA showed efficacy as an anti-inflammatory treatment when used as a prophylactic treatment in a mouse RA model [37], thus the increased peroxidation of DHA catalysed by ROS reduces the body's anti-inflammatory capacity. Oxidative stress has been identified as an aggravator of damage caused to bone in cartilage in RA [38, 39], so its correlation with CRP underscores this relationship.

DAS28 is the most widely used measurement for assessing the disease activity (swelling and tenderness in 28 joints, the ESR and VAS general health) in RA [40]. In the present study, good responders had higher baseline DAS28 compared with non-responders. Clinically, it has been observed that a patient with severe RA has high DAS28 and is more likely to obtain therapeutic response [41]. Veselinovic et al. reported increased levels of RNS in patients with high disease activity in serum [38], while we found in urine that the downstream anti-inflammatory  $\text{NO}_2$ -FAs correlated negatively with DAS28. This observation could be explained through the complex relationship between RNS species, the beneficial signalling abilities of RNS-nitrated lipid metabolites ( $\text{NO}_2$ -FAs) and the body's anti-oxidant capacity. The positive correlation of DAS28 improvement with strong pro-inflammatory mediators  $\text{PGF}_{2\alpha}$ ,  $\text{PGF}_{3\alpha}$  and oxidative stress markers  $\text{iPF}_{2\alpha}$ -IV, 11-HETE and 14-HDoHE indicates the higher disease burden within these baseline patients. The correlation of DAS28 and its improvement with the anti-inflammatory CYP-450

dihydroxy-fatty acids metabolites and the LOX derived  $\text{LXA}_4$  possibly reflects the intact innate anti-inflammatory pathways in these patients still trying to lessen the RA disease burden. The dihydroxy-fatty acids, 14,15-DiHETE, 11,12-EpETrE and 14,15-DiHETrE are able to attenuate pro-inflammatory pathways through activating and signalling via the PPAR-gamma pathway [42]. The urinary oxidised lipid profile of RA patients indicates the complex nature of the disease with oxidative stress and inflammation having an intimate relationship with clinically measured parameters.

## Conclusions

In the present study, we thoroughly explored different deglucuronidation methods for urinary oxidised lipids and developed a bovine liver GUS hydrolysing sample preparation method coupled with LC-MS to analyse the total urinary oxidised lipid profile. With bovine liver GUS hydrolysis, we are able to zoom into the urinary oxidised lipid metabolome, providing a readout for inflammation and oxidative stress. Our method detected more than 70 oxidised lipids in urine samples, biosynthesised from two non-enzymatic and three enzymatic pathways. The total oxidised lipid profiling method was developed and validated for human urine and was demonstrated on patients with RA. The urinary oxidised lipid profile of RA patients indicates the complex nature of the disease with oxidative stress and inflammation having an intimate relationship with clinically measured parameters. In conclusion, the hydrolysed method developed here allows specific and sensitive quantitative assessment of more than 70 oxidised lipids, which expands the scope of compounds in urinary metabolic profiling and may have wider applications in studies elucidating the role of these potent bioactive metabolites in human diseases.

**Acknowledgements** The authors express their gratitude to the people from the University Medical Centre Utrecht for providing the samples of BioCURA. The authors thank L. Lamont-de Vries for the help in sample analysis. The China Scholarship Council is also gratefully acknowledged (J. Fu, file number 201206200123). The funding provided by the Virgo consortium for J.C. Schoeman, funded by the Dutch government project number FES0908.

## Compliance with ethical standards

**Conflict of interest** The authors declare that they have no conflicts of interest.

**Open Access** This article is distributed under the terms of the Creative Commons Attribution 4.0 International License (<http://creativecommons.org/licenses/by/4.0/>), which permits unrestricted use, distribution, and reproduction in any medium, provided you give appropriate credit to the original author(s) and the source, provide a link to the Creative Commons license, and indicate if changes were made.

## References

- Montuschi P, Barnes PJ, Roberts LJ. Isoprostanes: markers and mediators of oxidative stress. *FASEB J*. 2004;18:1791–800. doi:10.1096/fj.04-2330rev.
- Milne GL, Yin H, Hardy KD, Davies SS, Roberts LJ. Isoprostane generation and function. *Chem Rev*. 2011;111:5973–96. doi:10.1021/cr200160h.
- Baker PRS, Schopfer FJ, Donnell VBO, Freeman BA. Convergence of nitric oxide and lipid signaling: anti-inflammatory nitro-fatty acids. *Free Radic Biol Med*. 2009;46:989–1003. doi:10.1016/j.freeradbiomed.2008.11.021.
- Richelle M, Turini ME, Guidoux R, Tavazzi I, Métaïron S, Fay LB. Urinary isoprostane excretion is not confounded by the lipid content of the diet. *FEBS Lett*. 1999;459:259–62. doi:10.1016/S0014-5793(99)01259-4.
- Galano J-M, Lee YY, Durand T, Lee JC-Y. Special issue on “analytical methods for oxidized biomolecules and antioxidants” the use of isoprostanooids as biomarkers of oxidative damage, and their role in human dietary intervention studies. *Free Radic Res*. 2015;49:583–98. doi:10.3109/10715762.2015.1007969.
- Buczynski MW, Dumlao DS, Dennis EA. Thematic review series: proteomics. An integrated omics analysis of eicosanoid biology. *J Lipid Res*. 2009;50:1015–38. doi:10.1194/jlr.R900004-JLR200.
- Stables MJ, Gilroy DW. Old and new generation lipid mediators in acute inflammation and resolution. *Prog Lipid Res*. 2011;50:35–51. doi:10.1016/j.plipres.2010.07.005.
- Smyth EM, Grosse T, Wang M, Yu Y, FitzGerald GA. Prostanoids in health and disease. *J Lipid Res*. 2009;50:S423–8. doi:10.1194/jlr.R800094-JLR200.
- Serhan CN. Novel lipid mediators and resolution mechanisms in acute inflammation: to resolve or not? *Am J Pathol*. 2010;177:1576–91. doi:10.2353/ajpath.2010.100322.
- Tai HH, Ensor CM, Tong M, Zhou H, Yan F. Prostaglandin catabolizing enzymes. *Prostaglandins Other Lipid Mediat*. 2002;68–69:483–93. doi:10.1016/S0090-6980(02)00050-3.
- Stachulski AV, Meng X. Glucuronides from metabolites to medicines: a survey of the in vivo generation, chemical synthesis and properties of glucuronides. *Nat Prod Rep*. 2013;30:806–48. doi:10.1039/c3np70003h.
- Trontelj J (2012) Quantification of glucuronide metabolites in biological matrices by LC-MS/MS. *Tandem Mass Spectrom Appl Princ* 531–558. doi: 10.5772/30923
- Prakash C, Zhang JY, Falck JR, Chauhan K, Blair IA. 20-Hydroxyeicosatetraenoic acid is excreted as a glucuronide conjugate in human urine. *Biochem Biophys Res Commun*. 1992;185:728–33. doi:10.1016/0006-291X(92)91686-K.
- Schwartz MS, Desai RB, Bi S, Miller AR, Matuszewski BK. Determination of a prostaglandin D2 antagonist and its acyl glucuronide metabolite in human plasma by high performance liquid chromatography with tandem mass spectrometric detection—a lack of MS/MS selectivity between a glucuronide conjugate and a phase. *J Chromatogr B Anal Technol Biomed Life Sci*. 2006;837:116–24. doi:10.1016/j.jchromb.2006.04.022.
- Yan Z, Mas E, Mori TA, Croft KD, Barden AE. A significant proportion of F2-isoprostanes in human urine are excreted as glucuronide conjugates. *Anal Biochem*. 2010;403:126–8. doi:10.1016/j.ab.2010.04.016.
- Kamata T, Nishikawa M, Katagi M, Tsuchihashi H. Optimized glucuronide hydrolysis for the detection of psilocin in human urine samples. *J Chromatogr B*. 2003;796:421–7. doi:10.1016/j.jchromb.2003.08.030.
- Little JM, Kurkela M, Sonka J, Jääntti S, Ketola R, Bratton S, et al. Glucuronidation of oxidized fatty acids and prostaglandins B1 and E2 by human hepatic and recombinant UDP-glucuronosyltransferases. *J Lipid Res*. 2004;45:1694–703. doi:10.1194/jlr.M400103-JLR200.
- Tsujikawa K, Kuwayama K, Kanamori T, Iwata Y, Ohmae Y, Inoue H, et al. Optimized conditions for the enzymatic hydrolysis of glucuronide in human urine. *J Health Sci*. 2004;50:286–9.
- Campbell WB, Holland OB, Adams BV, Gomez-Sanchez CE. Urinary excretion of prostaglandin E2, prostaglandin F2 alpha, and thromboxane B2 in normotensive and hypertensive subjects on varying sodium intakes. *Hypertension*. 2015;4:735–41.
- Mucha I, Riutta A. Determination of 9 alpha, 11 beta -prostaglandin F2 in human urine. Combination of solid-phase extraction and radioimmunoassay. *Prostaglandins Leukot Essent Fat Acids*. 2001;65:271–80. doi:10.1054/plef.2001.0325.
- Frölich JC, Wilson TW, Sweetman BJ, Smigel M, Nies AS, Carr K, et al. Urinary prostaglandins. Identification and origin. *J Clin Invest*. 1975;55:763–70. doi:10.1172/JCI107987.
- Newman JW, Watanabe T, Hammock BD. The simultaneous quantification of cytochrome P450 dependent linoleate and arachidonate metabolites in urine by HPLC-MS/MS. *J Lipid Res*. 2002;43:1563–78. doi:10.1194/jlr.D200018-JLR200.
- Sterz K, Scherer G, Ecker J. A simple and robust UPLC-SRM/MS method to quantify urinary eicosanoids. *J Lipid Res*. 2012;53:1026–36. doi:10.1194/jlr.D023739.
- Barocas DA, Motley S, Cookson MS, Chang SS, Penson DF, Dai Q, et al. Oxidative stress measured by urine F2-isoprostane level is associated with prostate cancer. *J Urol*. 2011;185:2102–7. doi:10.1016/j.juro.2011.02.020.
- Medina S, Domínguez-Perles R, Gil JI, Ferreres F, García-Viguera C, Martínez-Sanz JM, et al. A ultra-pressure liquid chromatography/triple quadrupole tandem mass spectrometry method for the analysis of 13 eicosanoids in human urine and quantitative 24 hour values in healthy volunteers in a controlled constant diet. *Rapid Commun Mass Spectrom*. 2012;26:1249–57. doi:10.1002/rcm.6224.
- Welsh TN, Hubbard S, Mitchell CM, Mesiano S, Zarzycki PK, Zakar T. Optimization of a solid phase extraction procedure for prostaglandin E2, F2alpha and their tissue metabolites. *Prostaglandins Other Lipid Mediat*. 2007;83:304–10. doi:10.1016/j.prostaglandins.2007.02.004.
- Yan W, Byrd GD, Ogden MW. Quantitation of isoprostane isomers in human urine from smokers and nonsmokers by LC-MS/MS. *J Lipid Res*. 2007;48:1607–17. doi:10.1194/jlr.M700097-JLR200.
- Medina S, Domínguez-Perles R, Cejuela-Anta R, Villaño D, Martínez-Sanz JM, Gil P, et al. Assessment of oxidative stress markers and prostaglandins after chronic training of triathletes. *Prostaglandins Other Lipid Mediat*. 2012;99:79–86. doi:10.1016/j.prostaglandins.2012.07.002.
- Nair SC, Welsing PMJ, Marijnissen AKCA, Sijtsma P, Bijlsma JWI, van Laar JM, et al. Does disease activity add to functional disability in estimation of utility for rheumatoid arthritis patients on biologic treatment? *Rheumatology (Oxford)*. 2016;55:94–102. doi:10.1093/rheumatology/kev291.
- Taylor JI, Grace PB, Bingham S a. Optimization of conditions for the enzymatic hydrolysis of phytoestrogen conjugates in urine and plasma. *Anal Biochem*. 2005;341:220–9. doi:10.1016/j.ab.2005.03.053.
- Gomes RL, Meredith W, Snape CE, Sephton MA. Analysis of conjugated steroid androgens: deconjugation, derivatisation and associated issues. *J Pharm Biomed Anal*. 2009;49:1133–40. doi:10.1016/j.jpba.2009.01.027.
- Strassburg K, Huijbrechts AML, Kortekaas KA, Lindeman JH, Pedersen TL, Dane A, et al. Quantitative profiling of oxylipins through comprehensive LC-MS/MS analysis: application in cardiac surgery. *Anal Bioanal Chem*. 2012;404:1413–26. doi:10.1007/s00216-012-6226-x.

33. Linting M, van der Kooij A. Nonlinear principal components analysis with CATPCA: a tutorial. *J Pers Assess.* 2012;94:12–25. doi:10.1080/00223891.2011.627965.
34. Shannon P, Markiel A, Ozier O, Baliga NS, Wang JT, Ramage D, et al. Cytoscape: a software environment for integrated models of biomolecular interaction networks. *Genome Res.* 2003;13:2498–504. doi:10.1101/gr.1239303.
35. Peters FT, Remane D. Aspects of matrix effects in applications of liquid chromatography-mass spectrometry to forensic and clinical toxicology—a review. *Anal Bioanal Chem.* 2012;403:2155–72. doi:10.1007/s00216-012-6035-2.
36. Salvatore SR, Vitturi DA, Baker PRS, Bonacci G, Koenitzer JR, Woodcock SR, et al. Characterization and quantification of endogenous fatty acid nitroalkene metabolites in human urine. *J Lipid Res.* 2013;54:1998–2009. doi:10.1194/jlr.M037804.
37. Olson MV, Liu YC, Dangi B, Paul Zimmer J, Salem N, Nauroth JM. Docosahexaenoic acid reduces inflammation and joint destruction in mice with collagen-induced arthritis. *Inflamm Res.* 2013;62:1003–13. doi:10.1007/s00011-013-0658-4.
38. Veselinovic M, Barudzic N, Vuletic M, Zivkovic V, Tomic-Lucic A, Djuric D, et al. Oxidative stress in rheumatoid arthritis patients: relationship to diseases activity. *Mol Cell Biochem.* 2014;391:225–32. doi:10.1007/s11010-014-2006-6.
39. Wruck C, Fragoulis A, Gurzynski A, Brandenburg L, Kan Y, Chan K, et al. Role of oxidative stress in rheumatoid arthritis: insights from the Nrf2-knockout mice. *Ann Rheum Dis.* 2011;70:844–50.
40. Prevoo M, van 't Hof M, Kuper H, van Leeuwen M, van de Putte L, van Riel P. Modified disease activity scores that include twentyeight-joint counts: development and validation in a prospective longitudinal study of patients with rheumatoid arthritis. *Arthritis Rheum.* 1995;38:44–8.
41. Isaacs JD, Ferraccioli G. The need for personalised medicine for rheumatoid arthritis. *Ann Rheum Dis.* 2011;70:4–7. doi:10.1136/ard.2010.135376.
42. Thomson SJ, Askari A, Bishop-Bailey D. Anti-inflammatory effects of epoxyeicosatrienoic acids. *Int J Vasc Med.* 2012;2012:1–7. doi:10.1155/2012/605101.